Transportation Research Part F: Psychology and Behaviour xxx (xxxx) 1–17

Contents lists available at ScienceDirect

Transportation Research Part F: Psychology and Behaviour

journal homepage: www.elsevier.com/locate/trf

Car sickness in real driving conditions: Effect of lateral acceleration and predictability reflected by physiological changes

Eléonore H. Henry [a, b, *], Clément Bougard [a, b], Christophe Bourdin [b], Lionel Bringoux [b]

[a] Stellantis, Centre Technique de Vélizy, Vélizy-Villacoublay, France
[b] Aix Marseille Univ, CNRS, ISM, Marseille, France

ARTICLE INFO

Keywords:
Lateral acceleration
Predictability
Physiological measures
Car sickness
Real driving

ABSTRACT

With the development of autonomous vehicles, car sickness may affect increasing numbers of car occupants. Car manufacturers have a real need to understand the causes of these symptoms, which occur mainly when car occupants are not engaged in a driving task. This study is the first to evaluate, in real driving conditions, the impact of lateral acceleration level and vehicle path predictability on car sickness incidence and severity, and the potential relationship with physiological changes. 24 healthy volunteers participated as front seat passengers in a slalom session inducing lateral movements at very low frequency (0.2 Hz). They were continuously monitored via physiological recordings and provided subjective car sickness ratings (CSR) after each slalom, using a 5-point likert scale. CSR reveal that (i) the greater the lateral acceleration and (ii) the less predictable the vehicle path, the more severe the car sickness symptoms in real driving conditions. An increase in several physiological parameters is also found simultaneously with higher CSR, demonstrating activation of the sympathetic nervous system. Moreover, the linear regression applied to our data suggests that these physiological parameters can be used to indicate car sickness severity. Moreover, the linear regression applied to our data suggests that the evolution of these physiological parameters may reflect the CSR level indicated by participants.

1. Introduction

Car sickness is very common, affecting about 60 % of the population (Diels, 2014), mainly passengers, half of whom present high susceptibility and severe symptoms (Rolnick & Lubow, 1991; Chen et al., 2010; Bos et al., 2018). Indeed, exposure to certain car motion can lead to car sickness symptoms ranging from mild stomach aches or headaches to dizziness, nausea, and ultimately vomiting (Dennison et al., 2016; Green, 2016). However, the development of autonomous vehicles, turning drivers into passengers (Sivak & Schoettle, 2015; Diels & Bos, 2016; Kuiper, Bos, Diels, et al., 2020a), should sharply increase the numbers exposed to car sickness (Diels, 2014; Kuiper et al., 2018). This would run counter to the promise of enhanced driver comfort during transport (Diels & Bos, 2016; Salter et al., 2019). Thus, understanding what induces these symptoms is currently a major concern for car manufacturers, particularly when the car occupant is not engaged in a driving task.

* Corresponding author: 163, av. de Luminy F, 13288 Marseille cedex 09, France.
E-mail addresses: eleonorehenry96@gmail.com (E.H. Henry), clement.bougard@stellantis.com (C. Bougard), christophe.bourdin@univ-amu.fr (C. Bourdin), lionel.bringoux@univ-amu.fr (L. Bringoux).

https://doi.org/10.1016/j.trf.2023.06.018
Received 18 December 2022; Received in revised form 26 June 2023; Accepted 27 June 2023
1369-8478/

Studies with this objective have so far been mainly conducted in laboratories, rarely in real vehicles. However, it was demonstrated that the sensory context induced by laboratory stimuli will always diverge from that in a real car (Mühlbacher et al., 2020). For example, when a rotating chair is used, the stimuli are mainly force-related, inducing vestibular and somatosensory solicitations which may cause some motion sickness (eg. coriolis or somatogyral illusions (Lackner, 2014)). Conversely, with a virtual reality headset, the stimuli are only visual, leading to visually-induced motion sickness (VIMS) (Naqvi et al., 2015; Dennison et al., 2016; Kim & Park, 2020). Some attempts have been made to create a more realistic driving environment using dynamic driving simulators (combination of virtual reality + physical motion) (Lin et al., 2007; Chen et al., 2010; Aykent et al., 2014). While this has the advantage of engaging multimodal sensory inputs, the latter can never precisely replicate cars' movements (Mühlbacher et al., 2020). Therefore, no consensus on the exact origins of car sickness has been reached, principally due to the diversity of conditions and stimuli used in these studies.

Studies on motion sickness tend to focus first on the vertical movements very common in situations inducing sea sickness and air sickness. The characteristics of the motion itself (e.g. acceleration, frequency, duration, speed, axis, etc.) are known to influence the occurrence and severity of motion sickness (Lawther & Griffin, 1987; Bos & Bles, 1998; Koohestani et al., 2019). Movements at very low frequency induce symptoms, especially when oscillating between 0.10 and 0.50 Hz (Turner, 1999; Golding et al., 2001; Donohew & Griffin, 2004; Cheung & Nakashima, 2006). In laboratory conditions investigating vertical movements, pioneering modeling work identified a critical threshold between 0.16 and 0.20 Hz inducing the highest incidence of motion sickness (O'Hanlon & McCauley, 1974). Since inertial forces tend to be interpreted by the vestibular system as translational above 0.20 Hz and as tilt below this value, such a frequency should be sufficient to create strong intravestibular conflict (Bos & Bles, 1998). In addition, Lawther and Griffin (1987) found a linear relationship between the magnitude of vertical accelerations on ships and the incidence of motion sickness (MSI). With a range of 0.0 to 5.4 m/s2, an adapted McCauley's (1974) model showed a sigmoidal relationship between vertical acceleration magnitude and MSI: the greater the vertical acceleration, the more rapid the onset and the more severe the symptoms (O' Hanlon & McCauley, 1974; Bos & Bles, 1998). In cars, however, horizontal accelerations caused by braking (longitudinal) and turning (lateral) were shown to play a greater role in sickness incidence than vertical accelerations (Cheung & Nakashima, 2006; Diels, 2014). A recent systematic review (Schmidt et al., 2020) found that the triggers of car sickness most frequently cited were those involving repeated lateral acceleration (multiple turns [71.8 %], winding roads [70.5 %]). It is actually lateral motion at very low frequency, around 0.2 Hz, that was found to be the principal component of car sickness (Wada & Yoshida, 2016; Kuiper et al., 2018; Henry et al., 2022). Strikingly however, no study so far has specifically investigated the impact of different levels of lateral acceleration on car sickness severity in real driving conditions.

For car manufacturers, there is another key issue: the difference in passengers' and drivers' susceptibility to car sickness. This difference mainly arises from the driver's ability to control and anticipate vehicle paths (Griffin & Newman, 2004; Perrin et al., 2013; Wada & Yoshida, 2016). Conversely, passengers are passively exposed to vehicle motion and have a limited knowledge of forthcoming actions (e.g., direction, speed, strength, duration etc.). Several studies conclude that the ability to predict future movements may reduce the level of motion sickness induced (Rolnick & Lubow, 1991; Feenstra et al., 2011; Levine et al., 2014). These observations are supported by the theory of sensory mismatch, which occurs when perceptual expectations from the internal model about upcoming sensory inputs do not match those actually perceived (Reason, 1978; Dennison et al., 2016). In other words, passengers may experience discrepancies between their expectations and reality, whereas drivers planning their driving control actions can precisely anticipate vehicle motion (Griffin & Newman, 2004; Perrin et al., 2013; Wada et al., 2018). In addition, the magnitude of this discrepancy seems to impact the symptom severity of motion sickness (Dennison et al., 2016; Kuiper, Bos, Schmidt, et al., 2020b). While sensory mismatch is often suggested as a cause of car sickness, however, less is known about how vehicle path unpredictability may affect car sickness severity in real driving conditions.

Accurate analysis of the impact of each factor inducing motion sickness requires a method of identifying and assessing the symptoms. Currently, the most widely used are questionnaires (MSSQ (Golding, 2006); MSAQ (Gianaros et al., 2003); SSQ (Kennedy, 1993) etc.) and subjective scales (MISC (Bos et al., 2006); Griffin and Newman's scale, (2004) etc.). However, both depend on the individual's subjective feelings and on how the individual interprets the scale in reporting discomfort. Moreover, both tools suffer from low temporal and sickness resolution (Irmak, 2021). There is clearly a need for a more reliable and objective method of measuring motion sickness severity.

Given the nature of the symptoms observed, physiological indicators could be a promising complement. In fact, motion sickness is considered a neuro-vegetative crisis that can initiate physiological changes, also commonly observed during stressful events (Money, 1970; Gianaros et al., 2003; Muth, 2006). Attempts have been made to identify these changes for an objective measure of motion sickness, by exploring several physiological variables: electrocardiography (ECG), respiration (RSP), electrodermal activity (EDA), electrogastrogram (EGG), and electroencephalography (EEG). Multiple features have been extracted from each variable, most commonly: heart rate (HR) and heart rate variability (HRV) for ECG, breathing rate (BR) for RSP, mean skin conductance level (SCL) and response (SCR) for EDA, stomach contraction activity for EGG, and changes in frequency band content for EEG (Kim et al., 2005; Dahlman et al., 2009; Dennison et al., 2016; Koohestani et al., 2019; Henry et al., 2022). However, although most of the motion sickness studies were conducted in laboratory environments, their results were not consistent, possibly due to the wide variety of devices and stimuli used (Koohestani et al., 2019). For example, when measuring HR, some studies reported a decrease using a rotating optokinetic drum (Hu et al., 1991) and VIMS (VR (Nalivaiko et al., 2015; Dennison et al., 2016); Static driving simulator (Kim et al., 2005)), while others found an increase in HR with similar devices but different stimuli (rotating optokinetic drum (Dahlman et al., 2009); VR (Cheung, 2004; Himi et al., 2004). Between-study discrepancies in results were also observed for HRV, BR, and EDA measurements (Hu et al., 1991; Kim et al., 2005; Dahlman et al., 2009; LaCount et al., 2009; Nalivaiko et al., 2015; Dennison et al., 2016; Gavgani et al., 2017; Islam et al., 2020). Where car sickness symptoms are evaluated in real driving conditions, only one study mea-

sures physiological variables (Irmak, 2021), with results indicating a clear link between EDA features and symptom severity, as well as a slight increase in HR. It has been suggested that depending on the environments, stimuli, and induced movements, the nervous system may be stimulated to a variable degree (Harm, 2002). This could explain the divergence in physiological responses and the lack of consensus on the indicators that can be considered predictive of motion sickness.

Individual reactions to motion thus vary in intensity and complexity with the movements to which participants are exposed. Seeking a more realistic assessment than that provided by laboratory conditions, this study was conducted in real car driving conditions using 0.2 Hz lateral movements. Our aim was to assess how (i) lateral acceleration level and (ii) ability to predict vehicle path impacted the severity of passengers' car sickness. Based on the literature, we hypothesized that (i) the stronger the acceleration, the more severe the symptoms and (ii) inability to predict vehicle path also exacerbates symptoms in real driving conditions. Another major objective was to relate possible physiological responses to car sickness and to determine which variables might indicate car sickness severity in real driving conditions. We hypothesized that (i) the parameters of interest for each measure (cardiac, respiratory, and electrodermal) would increase gradually throughout the stimulation, reflecting the activation of the sympathetic nervous system, (ii) each of these parameters would be impacted during the post-test period, and (iii) their respective evolution should be linked to increasing symptom severity.

2. Materials and methods

2.1. Participants

Twenty-four healthy right-handed volunteers (12 women and 12 men, mean age: 39.3 ± 9 years) with no neurological or vestibular disorders took part in the experiment, having drunk no stimulating or alcoholic drinks in the previous 24 h. Minimum age was 20 years, with a driver's license held for at least 2 years. As mentioned in the introduction, autonomous vehicles, by turning drivers into passengers, are likely to expose them to car sickness. Given that half the passengers affected by car sickness show high susceptibility, we therefore focused on this population (Bos et al., 2018). To guarantee sample homogeneity and limit inter-individual variability, participants were selected for their high susceptibility to motion sickness and car sickness, assessed by the Motion Sickness Susceptibility Questionnaire (mean percentile score: 90.6 ± 9.2 % (Golding, 2006)). Participants were informed of the study procedure and general objectives before signing a consent form warning them that they might experience car sickness during test sessions and that they could withdraw from the experiment at any time and for any reason. One participant became too sick to finish the experiment and quit the study. Participation was unpaid and no conflict of interest was declared. This study was approved by the local ethics committee of Aix-Marseille University in accordance with the ethical standards laid down in the 1964 Declaration of Helsinki.

2.2. General experimental set-up

Test sessions were conducted in a closed area approximately 400 m long and 50 m wide, with no other traffic present, for controllability and safety reasons. The vehicle used for these tests was a medium-sized car popular in France (Citroën C4 Picasso), driven by one professional driver specifically trained to produce reproducible vehicle dynamics for all participants. During the test session, participants were seated in the front passenger seat of the vehicle in a predefined sitting position, safety belt fastened. We focused on the front passenger position to replicate as closely as possible what happens when a driver becomes a passenger (in autonomous vehicles), mainly in terms of the visual and vestibular experience. Car ventilation and temperature were monitored to provide a similar controlled environment for each participant. They were continuously equipped with physiological modules for electrocardiogram (ECG), respiration (RSP), and electrodermal activity (EDA) recordings (detailed further). A slider was positioned in front of volunteers to allow them to indicate their car sickness level during every test period (equipment detailed below). For synchronization, data from the physiological modules, the car sickness rating slider, and the vehicle's Controller Area Network (CAN) were recorded by a laptop in the rear seat of the vehicle. The experimental road consisted of two straight segments approximately 300 m long with 10 m-radius turning zones at both ends, forming an oval track. Three rows of twelve pylons spaced 20 m apart were located along both straight segments, with a 6 m gap between rows (Fig. 1 - A).

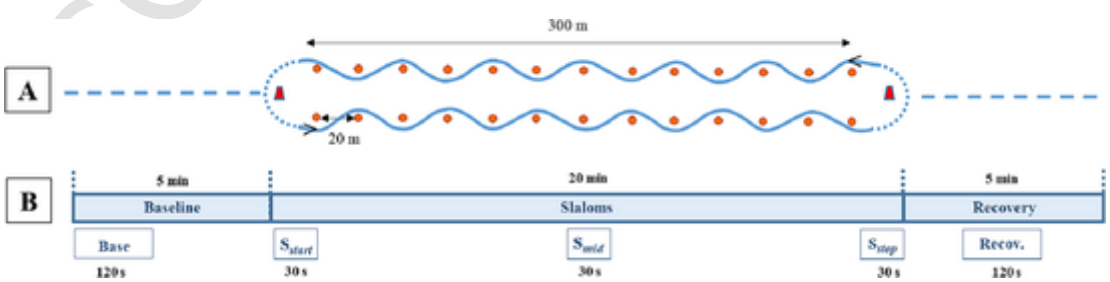

Fig. 1. Representation of **(A)** test set-up and timeline of the test session, in periods: baseline, slalom, recovery; **(B)** the five time intervals per session analyzed: baseline (Base), slaloms (comprising S_{start}, S_{mid}, $S_{stop,}$), and recovery (Recov). See Section 4 Data acquisition and processing.

2.3. Procedure

Every test session began with one baseline period of 5 min in the parked car, during which resting physiological recordings were collected and signal quality was assessed visually (online check). Next came a slalom period of about 20 min to induce car sickness symptoms. If participants felt too sick to finish the test (i.e., maximum rating of 4 on the discomfort scale), the slalom period was interrupted, and the vehicle was parked. Once the vehicle stopped, there was a static recovery period of 5 min. During all periods, participants were instructed to look frontwards and to move as little as possible. Each participant took part in two test sessions on the same day, with a one-hour lag between sessions, which lasted approximately 60 min (participant equipment, testing, and debriefing). At the end of their second test session, participants were given details of the study's objectives and thanked for volunteering.

During the slalom period, the car was driven at a continuous speed of about 35 km/h and, in order to minimize additional lateral acceleration, the speed was limited to about 15 km/h during U-turns. The gap between pylons and the car speed ensured lateral movements of close to 0.2 Hz, recognized as a car-sickness-inducing frequency (Bos & Bles, 1998).

Four conditions were designed to examine the effects of two independent variables. Two conditions assessed the influence of degree of lateral acceleration in regular slaloms, while two others assessed the influence of inability to predict vehicle path in both regular and unpredictable slaloms. The purely regular slalom conditions involved two levels of acceleration: high (5 m.s^2) called Regular High (RH) and low (2 m.s2) called Regular Low (RL) (Fig. 2). These acceleration levels were based on the McCauley (1974) vertical model: low acceleration (2 m/s2) causing 50 % of MSI and the model's highest acceleration (5 m/s2) causing maximum MSI (O' Hanlon & McCauley, 1974; Bos & Bles, 1998). During each regular slalom, the driver executed zigzags to the left and right of the pylons to induce reproducible lateral acceleration levels. In the unpredictable slalom conditions, the vehicle followed the path of a regular slalom but, at a given time, the driver added an unpredictable turn in an unexpected way. When the regular slalom path acceleration was high, the unpredictable turn was performed at low acceleration: this is termed the Unpredictable High (UH) condition. In conditions with low regular slalom path acceleration, the unpredictable turn was performed at high acceleration: the Unpredictable Low (UL) condition (Fig. 2). Each participant took part in both a regular and an unpredictable condition at the same acceleration level.

2.4. Data acquisition

2.4.1. CAN recordings

The vehicle's CAN data were recorded to obtain speed, lateral acceleration, and frequency of movement oscillations. Sampling frequency was set at 100 Hz. Each slalom (start and end) was automatically identified from the level of lateral acceleration, using MATLAB software (MathWorks, 2017).

2.4.2. Car sickness rating recordings

The test included regular subjective assessments of car sickness severity, used to analyze the evolution of symptoms from their very first occurrence and to compare it with the evolution of physiological recordings. To limit the time spent scoring, we therefore chose a short and continuous scale using a slider, which was easy to understand and to remember. Based on the first five levels of Griffin and Newman's scale (2004), a 5-point likert scale was defined, graduated from 0 to 4: 0 = No symptom, 1 = Any symptom, however slight, 2 = Mild symptoms, for example, stomach awareness but no nausea, 3 = Mild nausea, 4 = Mild to moderate nausea (Green, 2016; Wada & Yoshida, 2016). The field was divided into 4 equal segments only indicated by colored dots, so that the participants were guided in evaluating their discomfort without being influenced by numbers. Each color corresponded to a rating: green for 0, white for 1 and 2, orange for 3 and red for 4. Participants rated their car sickness level via the slider in front of them. Only one score was recorded for baseline and one for the recovery period. In the slalom period, during the U-turns that followed each slalom, participants were instructed to give their rating based on the worst symptoms they experienced in the slalom just completed. Thus, since a slalom lasted about 30 sec, a score was obtained every 30 sec during the slalom period. One advantage of this method lies in its immediate assessment of car sickness symptoms, without test interruption and with attention only diverted for a few seconds during U-turns (periods not analyzed).

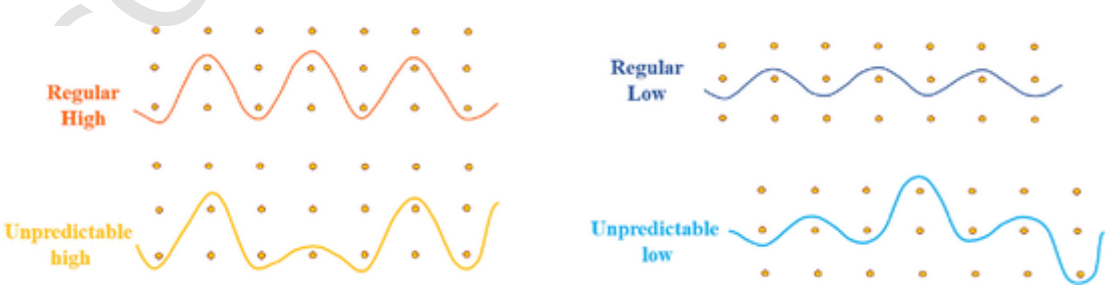

Fig. 2. Representations of the four experimental conditions assessing the influence of lateral acceleration (High vs Low conditions) and inability to predict vehicle path (Regular vs Unpredictable conditions).

2.4.3. Physiological recordings

Participants were continuously monitored to record physiological measurements with Bionomadix devices connected to a BIOPAC MP160 (BIOPAC Systems, Inc.). Physiological signals were amplified and recorded at a sample rate of 1000 Hz. Following a classical configuration, ECG was recorded with three disposable, pre-gelled Ag/AgCl 11 mm surface electrodes (EL503, BIOPAC Systems, Inc.) located on the left and right collarbone and in the 7th intercostal space. EDA was detected using two disposable, pre-gelled Ag/AgCl 11 mm electrodes (EL507, BIOPAC Systems, Inc.) placed on the index and middle finger of the non-dominant hand. This electrode location was chosen with a view to participants' comfort; moreover, several studies previously reported significant correlations between skin conductance recorded at the palmar finger site and motion sickness severity (Hu et al., 1991; Kim et al., 2005; LaCount et al., 2011; Sclocco et al., 2016; Irmak, 2021). RSP was recorded by a sensor band wrapped around the participant's chest (Fig. 3).

2.5. Physiological data processing

For data processing, six different phases of recordings common to all participants were selected for further analyses [(1) baseline (Base- first 120 s), (2) the first slalom (S_{start} – 30 s), (3) the middle slalom (S_{mid} – 30 s), (4) the last slalom (S_{stop} – 30 s), (5) the highest-CSR slalom (S_{max} – 30 s), and (6) recovery (Recov - middle 120 s) (Fig. 1 - B)]. Reference measurements were obtained from the baseline period. One car sickness rating was obtained for each slalom and each was linked to corresponding physiological recordings. For each participant, S_{max} was the highest car sickness level reported, as suggested by Chen et al. (2010) and Keshavarz et al. (2022). Finally, post-stimulation reactions were assessed via a rating recorded after 120 s of recovery.

Recording physiological parameters under ecological conditions is a technological challenge. A method of pre-processing and physiological feature extraction therefore had to be developed and adapted to our data, which contained more artifacts than average because of noise induced by the vehicle's and the participants' movements. This required several operations to obtain clean and useful signals. In addition, for the sake of clarity, only relevant physiological features were used. Our method involved the following steps.

2.5.1. Pre processing

Physiological raw signals were pre-processed on the selected periods of interest (Base, S_{start}, S_{mid}, $S_{max,}$ $S_{stop,}$ and Recov) (Fig. 1 - B). As physiological signals are time series, it is common to use wavelets to decompose them into frequency and time–frequency representations, with the wavelet coefficients chosen as characteristics (Shoeb & Clifford, 2005; Li & Chung, 2013; Pukhova et al., 2017). An advantage of wavelet features is their ability to encode a time and frequency resolution trade-off allowing signal responses to car sickness to be captured in different time windows. More specifically, we used soft and Daubechies 4 tap (Db4) wavelets obtained respectively from discontinuous and continuous base functions (Mother Wavelet: db4; Mode: Soft; Method: Sure Shrink; Level: 5). The chosen SureShrink method is an automatic procedure that, from decomposition coefficients at level 5, minimizes the unbiased estimate of mean square error. Once this step was completed, each physiological signal was filtered and cleaned using artifact removal techniques. Our method for ECG signals involved unsupervised artifact detection using an Isolation Forest model applied to 5-second signal intervals. Any abnormal intervals detected were replaced with the closest clean segment of the signal. To avoid overlap between the replaced signal and the PQRST waves in the previous and subsequent intervals, we applied two rules: i) if the interval between the two R waves was < 600 ms, one of the waves was removed; ii) if the interval between the two R waves was greater than 1100 ms, a new R wave was inserted between them (Salahuddin et al., 2007; Nunan et al., 2010). Furthermore, we used the Python NeuroKit library (Carreiras et al., 2015; Makowski, 2016) to apply two classical filtering methods addressing baseline slow drift and power line interference. More precisely, each ECG signal underwent 50 Hz power-line noise-filtering that involved smoothing the sig-

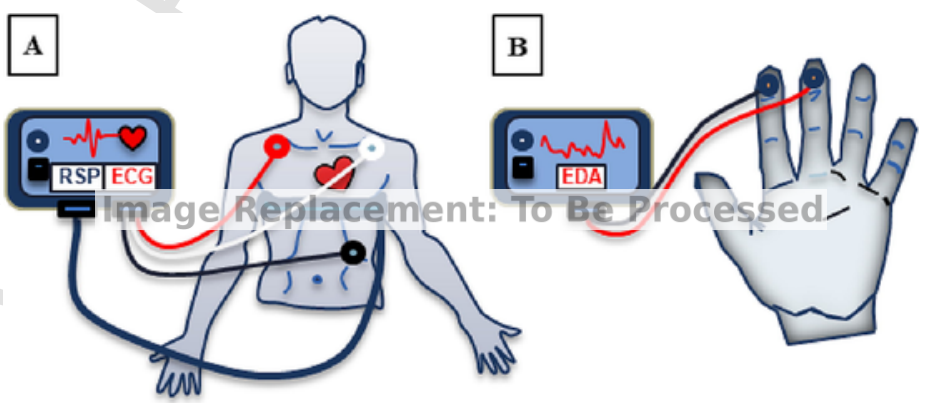

Fig. 3. Configuration of physiological measurement. **(A)** ECG and respiration belt measures: electrode configuration (white = VIN+, black = VIN-, red = ground) and position to obtain ECG. **(B)** EDA measures: electrode placement used to obtain EDA signals. The ground electrode (black) was placed on the middle finger and the active electrode (red) on the index finger on each participant's non-dominant hand. Leads (115 Series, BIOPAC Systems, Inc.) with light-weight pinch clips connected to thin wires were attached to all electrodes and plugged into wireless transmitters adhering to the chest (ECG, respiration belt) or wrist (EDA) of the participant. (For interpretation of the references to color in this figure legend, the reader is referred to the web version of this article.)

nal with a moving average kernel having a one-period width of 50 Hz. In addition, a Butterworth high pass filter with a cut-off frequency of 0.5 Hz was applied to remove baseline slow drifts. To process the respiratory signal, we applied a classical filtering technique using Python NeuroKit library (Carreiras et al., 2015; Makowski, 2016). A Butterworth band-pass filter with a low-cut frequency of 0.05 Hz and a high-cut frequency of 0.35 Hz was used to remove baseline drift and high frequency noise from the respiratory signal. Concerning EDA signals, supervised artifact removal was performed via an SVM-based model (Taylor et al., 2015). The binary model was already trained on a dataset of 5-second EDA signals labeled 'normal' or 'abnormal' (Taylor et al., 2015). We used this model on our EDA samples, replacing the artifacts by the mean of the current 5-second signal. In addition, any remaining artifacts were dealt with by a second removal applied to each 1-second signal interval via a second derivative model. Finally, the EDA signal underwent Butterworth low pass filtering at 3 Hz using Python NeuroKit library (Carreiras et al., 2015; Makowski, 2016).

2.5.2. Feature extraction

Once signals were pre-processed, physiological features were calculated from ECG, RSP, and EDA signals, using Python software (Python Software Foundation) with BioSPPy and NeuroKit libraries (Carreiras et al., 2015; Makowski, 2016). Features were computed for all signals on every 30-second window without overlapping. Key to ECG signal processing is analyzing and understanding the QRS complex waveform representing the ventricular depolarization (Yan et al., 2003). A QRS detection algorithm was used to extract ECG features using the BioSPPy library. We selected from the analyses performed slalom by slalom (30 s) the features mean heart rate ('Hr_mean') and standard deviation of heart rate ('Hr_std'); the other features depending on frequency domain analysis require longer temporal analysis windows and could not be calculated (60 s at least - Shaffer & Ginsberg, 2017). RSP features were calculated using the BioSPPy library, based on a detection algorithm for respiratory cycles, amplitudes, and phases (inspirations and expirations). Following the pre-test phase, it was observed that the frequency of the car movements at 0.2 Hz imposed a specific respiration rate, which is precisely why additional features not impacted by the car movements were calculated and investigated. With respiratory amplitude, the magnitude of each breathing phase was calculated by measuring the difference between the peak and trough of each breath in the respiration signal. Maximum inspiration ('In_max') and expiration ('Out_max') were chosen for analysis. The overall EDA signal was obtained from the fluctuation of two underlying components: one is a slower and steady baseline tonic component (skin conductance level (SCL)) and the other is a faster or reactive phasic component (skin conductance response (SCR)). Using the NeuroKit library, two SCR features were extracted through the phasic component: peak indexes and SCR amplitudes. SCR amplitude was a change relative to the deflection in the signal from onset to peak response. Mean SCR amplitude ('SCR_mean') and standard deviation ('SCR_std') were chosen for analysis. For each channel and feature, the mean and standard deviations were extracted over the different recording periods of interest to examine changes over time in the sample.

2.6. Statistical analysis

Several dependent variables were analyzed at full sample level: (i) car sickness ratings (CSR), (ii) features of the ECG recordings ('Hr_mean' and 'Hr_std'), (iii) features of the RSP recordings ('In_max' and 'Out_max'), and (iv) features of the SCR recordings ('SCR_mean' and 'SCR_std'). The evolution of each dependent variable was compared against three independent variables: 'acceleration level', 'path predictability', and 'period'. For the 'period' variable, 6 periods were defined: baseline period (Base), slalom period (S_{start}, S_{mid}, S_{stop} + S_{max}), and recovery period (Recov).

First, car sickness ratings and the time to reach maximum CSR were analyzed during the S_{max} period using a 2-level ('acceleration level': high and low) × 2-level ('path predictability': regular and unpredictable) repeated measures ANOVA. Secondly, the dynamics of changes in car sickness ratings and physiological features were analyzed using a 2-level ('acceleration level': high and low) × 2-level ('path predictability': regular and unpredictable) × 5-level ('period': Base, S_{start}, S_{mid}, S_{stop} and Recov) repeated measures ANOVA.

As a prior for all collected data, the condition of sphericity was also tested (Mauchly's test). The p-value levels were corrected for possible deviations from sphericity by means of the Huynh–Feldt epsilon (ε) (Kim et al., 2005; Ohyama et al., 2007; Benedek & Kaernbach, 2010; Dennison et al., 2016). When significant differences were observed ($p < 0.05$), post-hoc analysis was performed using a Fisher–Snedecor least significant difference test, allowing the results to be refined by comparing the modalities two by two. For each significant effect, the effect size was estimated using the partial eta squared (ηp^2).

Following these analyses, two-tailed Pearson correlation coefficients were calculated between physiological measurements and maximum CSR for all conditions. Physiological measurements were drawn from the S_{max} period and normalized from the Base period. Finally, stepwise multiple linear regression analysis was performed to determine which physiological changes contributed to the maximum CSR assessment. Only variables whose correlations with maximum CSR were greater than 0.2 were selected for regression analysis.

All statistical analyses were performed using Statistica software® v.10 (Statsoft Inc, France). Data are presented as mean ± SEM for each assessment and significance levels as $*p < 0.05$, $**p < 0.01$ and $***p < 0.001$.

3. Results

3.1. CAN recordings

All participants were subjected to a maximum of 26 slaloms during the slalom period. The mean time for one slalom, the mean time for the whole slalom period, and the mean of the resulting lateral oscillation frequencies and accelerations were calculated for each condition (Table 1).

3.2. Car sickness ratings (CSR)

3.2.1. Maximum CSR

During the test, all participants reported at least some degree of car sickness and reached their maximum CSR during the S_{max} period. The maximum ratings distribution for each condition is shown in Fig. 3. High conditions led to a distribution with more high scores (Bles et al., 1998; Bos and Bles, 1998) than Low conditions (RH: +75 % vs RL and UH: +39 % vs UL). Unpredictable conditions had a distribution with more high scores than Regular conditions for both acceleration levels (UH: +8 % vs RH and UL: +45 % vs RL) (Fig. 4). For an approximately similar level of acceleration (≈ 5 m.s²), there were more high scores in the UH condition than in the RH condition.

Table 1
Main characteristics of Regular Low (RL), Unpredictable Low (UL), Regular High (RH), and Unpredictable High (UH) slaloms experienced by the participants (mean ± SD). Note that the same ranges of mean lateral oscillation frequency and accelerations were applied in Regular and Unpredictable conditions.

Conditions	Mean time for 1 slalom (sec)	Mean time for slalom period (min)	Mean number of slaloms	Minimum number of slaloms	Lateral oscillation frequencies (Hz)	Lateral oscillation accelerations (m.s²)
Regular Low (RL)	32 ± 1	20 ± 1	26 ± 0.3	26	0.20 ± 0.04	2.0 ± 0.1
Unpredictable Low (UL)	32 ± 1	19 ± 3	25 ± 1.2	14	0.20 ± 0.04	3.0 ± 0.45
Regular High (RH)	35 ± 1	10 ± 7	13 ± 2.5	3	0.19 ± 0.04	5.5 ± 0.19
Unpredictable High (UH)	34 ± 1	11 ± 7	13 ± 2.9	2	0.19 ± 0.04	5.2 ± 0.28

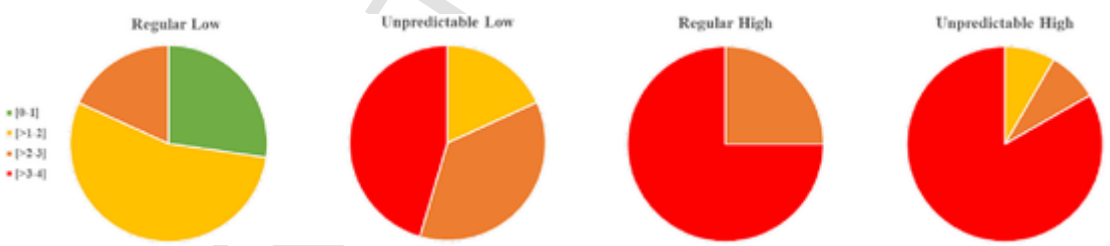

Fig. 4. Distribution of maximum CSR reached by participants during the S_{max} period: green [0–1], yellow [greater than1–2], orange [greater than2–3], and red [greater than3–4] (n = 23). (For interpretation of the references to color in this figure legend, the reader is referred to the web version of this article.)

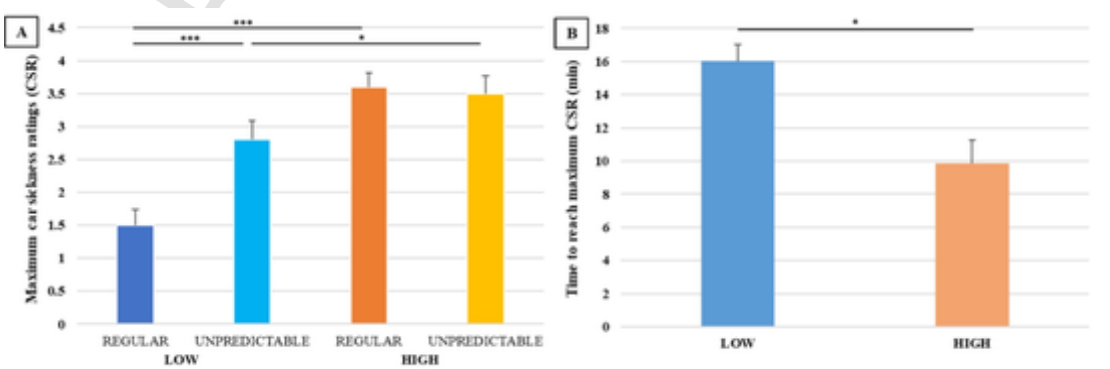

Fig. 5. (A) Maximum CSR observed for each condition in S_{max} period (B); time to reach maximum CSR (mean ± SEM; n = 23). Statistical differences between conditions are shown by black stars and full lines. * significant difference ($p < 0.05$), *** significant difference ($p < 0.001$).

Statistical analysis indicated a significant interaction effect between 'acceleration level' and 'path predictability' on maximum CSR measured in the S_{max} period ($F_{(1,21)} = 9.03$; $\varepsilon = 1.0$; $p < 0.01$; $\eta p^2 = 0.30$). Post-hoc analyses revealed higher ratings in High conditions than in Low conditions ($p < 0.001$) and higher ratings in UL than in RL ($p < 0.05$) (Fig 5 A). In addition, a significant effect of 'acceleration level' was observed on the time taken to reach maximum CSR ($F_{(1,21)} = 7.09$; $\varepsilon = 1.0$; $p < 0.05$; $\eta p^2 = 0.25$). Participants reached their maximum score faster in High conditions than in Low conditions (Fig 5 B). All results (mean ± SEM) obtained for each feature by test period (S_{max}, Base, S_{start}, S_{mid}, $S_{stop,}$ and Recov) can be found in supplementary material (Table 1). Details of all associated statistics are reported in Table 2 and supplementary material.

3.2.2. CSR dynamics

A significant interaction between 'test period', 'acceleration level', and 'path predictability' was observed on car-sickness rating dynamics ($F(3,63) = 5.61$; $\varepsilon = 0.91$; $p < 0.01$; $\eta p2 = 0.49$). Post-hoc analyses revealed that 'Base' and 'S_{start}' were not significantly affected. As illustrated in Fig. 6, each participant began the experiment symptom-free ('Base') and ratings did not significantly differ between conditions at 'S_{start}'. However, during the slalom period, ratings increased more or less sharply depending on conditions. There were significant differences between Low and High conditions ($p < 0.001$), with significantly higher ratings at 'S_{mid}', 'S_{stop}', and 'Recov' in the High conditions than in the Low conditions. In addition, there were significant differences between Regular and Unpredictable conditions ($p < 0.05$) (Table 2 and Supplementary material). Ratings were significantly higher at 'S_{mid}' and 'S_{stop}' in the UL conditions than in the RL conditions, and were also higher at 'S_{mid}' in the UH conditions than in the RH conditions (Table 2 and Supplementary material). Whatever the condition, none of the ratings returned to baseline level at 'Recov'.

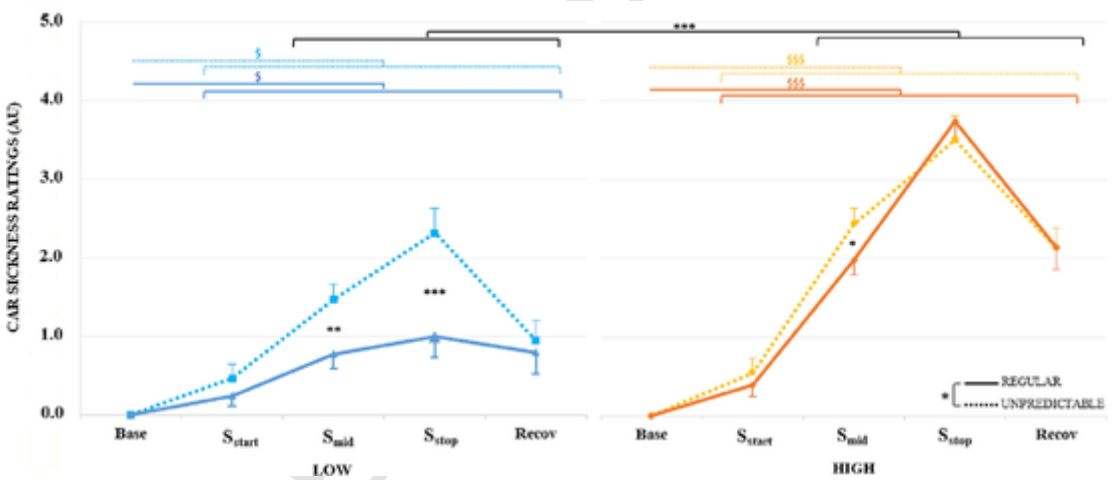

Fig. 6. CSR observed for each test period (Base, S_{start}, S_{mid}, $S_{stop,}$ and Recov) in each condition (mean ± SEM; n = 23). Statistical differences between test periods in a condition are shown by dollar symbols and lines color-coded by condition: (i) Regular Low: dark blue solid line, (ii) Unpredictable Low: light blue dashed line, (iii) Regular High: dark orange solid line, and (iv) Unpredictable High: light orange dashed line. Statistical differences between conditions are shown by black stars and full lines. * and $ significant difference ($p < 0.05$), ** significant difference ($p < 0.01$), *** and $$$ significant difference ($p < 0.001$). (For interpretation of the references to color in this figure legend, the reader is referred to the web version of this article.)

Table 2
Results of ANOVA analysis for each feature and each test period (Base, S_{start},S_{mid}, $S_{stop,}$ and Recov) in each condition (mean ± SEM; n = 23). The three independent variables are: ACCEL = acceleration level, PATH = path predictability, and PERIOD = test period.

Three-factor ANOVA							
	ACCEL	**PATH**	**PERIOD**	**PATH*ACCEL**	**PERIOD*ACCEL**	**PATH*PERIOD**	**PATH*PERIOD*ACCEL**
CSR	F(1,21)	F(1,21)	F(3.63)	F(1.21)	F(3.63)	F(3.63)	F(3.63)
	20.19***	9.08**	60.45***	4.76*	10.60***	2.90*	5.61**
	F(1,21)	F(1,21)	F(4.84)	F(1.21)	F(4.84)	F(4.84)	F(4.84)
HR_mean	0.00	0.17	20.02***	0.28	5.60***	3.41*	1.04
HR_std	1.65	0.61	2.44	0.60	3.21*	1.04	0.72
In_max	9.44**	2.50	17.34***	9.22**	3.60**	1.47	1.71
Out_max	9.00**	2.60	20.65***	9.55**	5.42***	3.13*	3.64**
SCR_mean	0.06	1.91	4.87**	0.43	1.92	1.05	0.47
SCR_std	0.65	3.93	6.51***	0.51	0.27	0.26	1.03

3.3. Physiological measurements

3.3.1. 'Hr_mean' dynamics

A significant interaction between 'test period' and 'acceleration level' was observed on mean heart rate ('Hr_mean') values ($F(4,84) = 5.56$; $\varepsilon = 0.46$; $p < 0.01$; $\eta p2 = 0.21$). Post-hoc analyses revealed a significant increase in all values during the slalom period compared to baseline (Fig. 7A). During the recovery period, only Low condition values returned to baseline level (Table 2 and Supplementary material). Another significant interaction was observed between 'test period' and 'path predictability' on mean heart rate ('Hr_mean') values ($F(3,63) = 5.61$; $\varepsilon = 0.36$; $p < 0.05$; $\eta p2 = 0.14$). Post-hoc analyses revealed a significant increase in all values during the slalom period compared to baseline (Fig. 7B). In addition, there was a significant difference between Regular and Unpredictable conditions for the recovery period ($p < 0.01$) (Table 2 and Supplementary material), with higher values in Unpredictable conditions than in Regular conditions. Only Regular condition values returned to baseline level.

3.3.2. 'Hr_std' dynamics

A significant interaction between 'test period' and 'acceleration level' was observed for standard deviation of the heart rate ('Hr_std') values ($F(4,84) = 3.21$; $\varepsilon = 0.40$; $p < 0.05$; $\eta p2 = 0.07$) (Table 2). For the High conditions, post-hoc analyses revealed a significant increase during the slalom period compared to baseline ($p < 0.01$) (Fig. 8 and Supplementary material). During Recov, values returned to baseline level (Supplementary Table 1).

3.3.3. 'In_max' dynamics

A significant interaction between 'acceleration level' and 'path predictability' was observed for maximum inspiration ('In_max') values ($F(1,21) = 9.22$; $\varepsilon = 0.96$; $p < 0.01$; $\eta p2 = 0.30$) (Table 2). Post-hoc analyses revealed higher values in the RH conditions than in the others (Fig. 9 and Supplementary material). There was another significant effect of interaction between 'test period' and 'acceleration level' on maximum inspiration ('In_max') values ($F(4,84) = 3.60$; $\varepsilon = 0.82$; $p < 0.01$; $\eta p^2 = 0.15$). For both acceleration levels (Low and High), post-hoc analyses revealed a significant increase in all values during the slalom period compared to baseline (Fig. 9). The increase was significantly higher in High conditions than in Low conditions for all slalom periods; values were also higher during the recovery period in High than in Low conditions. In High conditions, the values peaked at 'S_{stop}' and decreased during Recov but remained higher than baseline values. In Low conditions, no difference between slalom periods (S_{start}, S_{mid}, S_{stop}) was observed but values returned to baseline level during Recov.

3.3.4. 'Out_max' dynamics

A significant effect of interaction between 'test period', 'acceleration level', and 'path predictability' was observed on maximum expiration ('Out_max') values ($F(4,84) = 3.64$; $\varepsilon = 1.0$; $p < 0.01$; $\eta p2 = 0.30$). Post-hoc analyses revealed that 'Base' values were not significantly affected by the factors (Fig. 10). In contrast, during the slalom period, all values increased similarly compared to baseline, except in RH conditions, where significantly higher values were observed during slaloms and Recov than in the other conditions (Table 2 and Supplementary material). During Recov, only RH condition values did not return to baseline level.

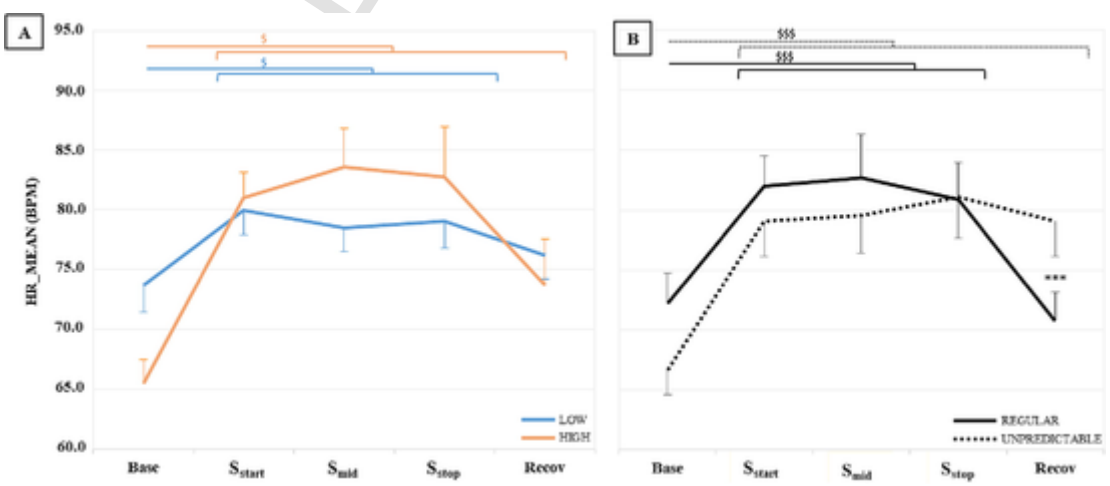

Fig. 7. Representation of 'HR_mean' values (mean ± SEM; n = 23) for (A) interaction between 'test period' and 'acceleration level' and (B) interaction between 'test period' and 'path predictability' in each test period (Base, S_{start}, S_{mid}, S_{stop} and Recov). Statistical differences between test periods in a condition are shown by dollar symbols and lines color-coded by condition: (i) Regular: black full line, (ii) Unpredictable: black dashed line, (iii) Low: light blue full line, and (iv) High: light orange full line. Statistical differences between conditions are shown by black stars. * and $ significant difference ($p < 0.05$), *** and $$$ significant difference ($p < 0.001$). (For interpretation of the references to color in this figure legend, the reader is referred to the web version of this article.)

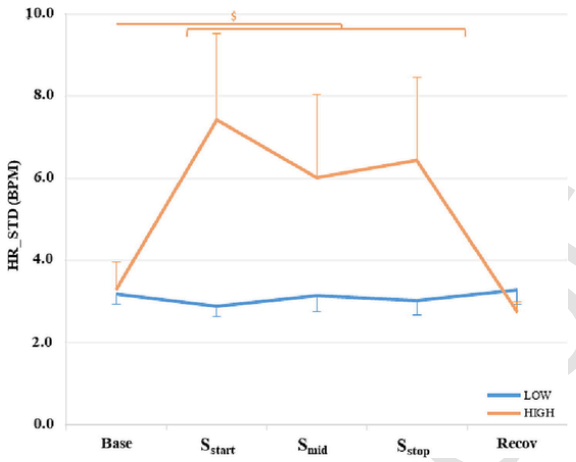

Fig. 8. 'Hr_std' values observed for each test period (Base, S_{start}, S_{mid}, S_{stop} and Recov) according to 'acceleration level', regardless of 'path predictability' (mean ± SEM; High conditions n = 12; Low conditions n = 11). Statistical differences between test periods in High conditions are indicated by a light orange dollar symbol and full lines. $ significant difference ($p < 0.05$). (For interpretation of the references to color in this figure legend, the reader is referred to the web version of this article.)

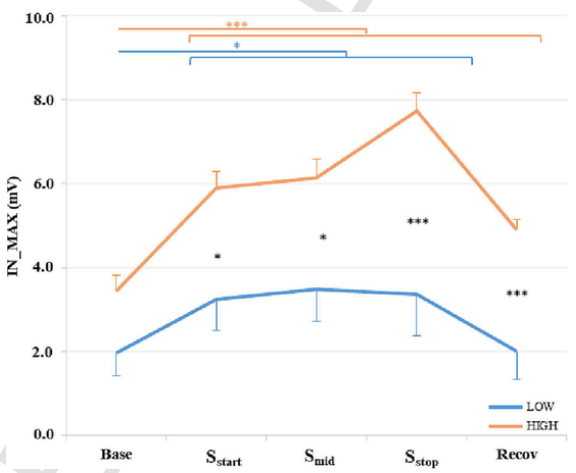

Fig. 9. 'In_max' values observed for each test period (Base, S_{start}, S_{mid}, S_{stop} and Recov) according to acceleration level, regardless of path predictability (mean ± SEM; High conditions n = 12; Low conditions n = 11). Statistical differences between test periods in a condition are shown by dollar symbols and lines color-coded by condition: (i) Low: light blue full line and (ii) High: light orange full line. Statistical differences between conditions are shown by black stars. * and $ significant difference ($p < 0.05$), *** and $$$ significant difference ($p < 0.001$). (For interpretation of the references to color in this figure legend, the reader is referred to the web version of this article.)

3.3.5. 'SCR_mean' dynamics

A significant main effect of 'test period' was observed on mean values for skin conductance response ('SCR_mean') ($F(4, 84) = 4.87$; $\varepsilon = 0.71$; $p < 0.01$; $\eta p2 = 0.19$). Post-hoc analyses revealed a significant increase during S_{mid} and S_{stop} compared to baseline (Fig. 11 A and Supplementary material). Finally, stopping the slalom during Recov induced a significant decrease in values, which returned to baseline level.

3.3.6. 'SCR_std' dynamics

A significant effect of 'test period' was observed on the standard deviation of skin conductance response ('SCR_std') ($F(4, 84) = 6.51$; $\varepsilon = 0.91$; $p < 0.001$; $\eta p2 = 0.24$). Post-hoc analyses revealed significant increases throughout the slalom period compared to baseline (Fig. 11 B and Supplementary material). Stopping the slalom during Recov induced a significant decrease in values, which returned to baseline level.

3.4. Relationship between car sickness ratings and physiological measurements

Significant correlations were observed between maximum CSR (CSR_max) and physiological parameters (Table 3A). There were significant correlations between CSR_max and 'HR_mean' and 'Out_max' values (greater than 0.4 for both), as well as with 'HR_std',

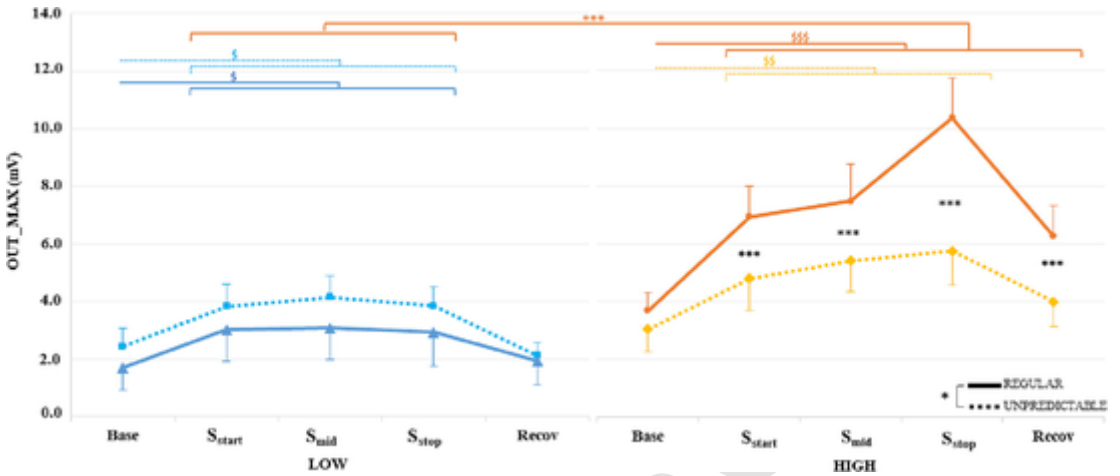

Fig. 10. 'Out_max' values observed for each test period (Base, S_{start}, S_{mid}, S_{stop} and Recov) in each condition (mean ± SEM; n = 23). Statistical differences between test periods in a condition are shown by dollar symbols and lines color-coded by condition: (i) Regular Low: dark blue full line, (ii) Unpredictable Low: light blue dashed line, (iii) Regular High: dark orange full line, (iv) Unpredictable High: light orange dashed line. For the Regular High condition, statistical differences between test periods and from other conditions are shown by dark orange stars and full lines. Statistical differences between conditions are shown by black stars. * and $ significant difference ($p < 0.05$), ** and $$ significant difference ($p < 0.01$), *** and $$$ significant difference ($p < 0.001$). (For interpretation of the references to color in this figure legend, the reader is referred to the web version of this article.)

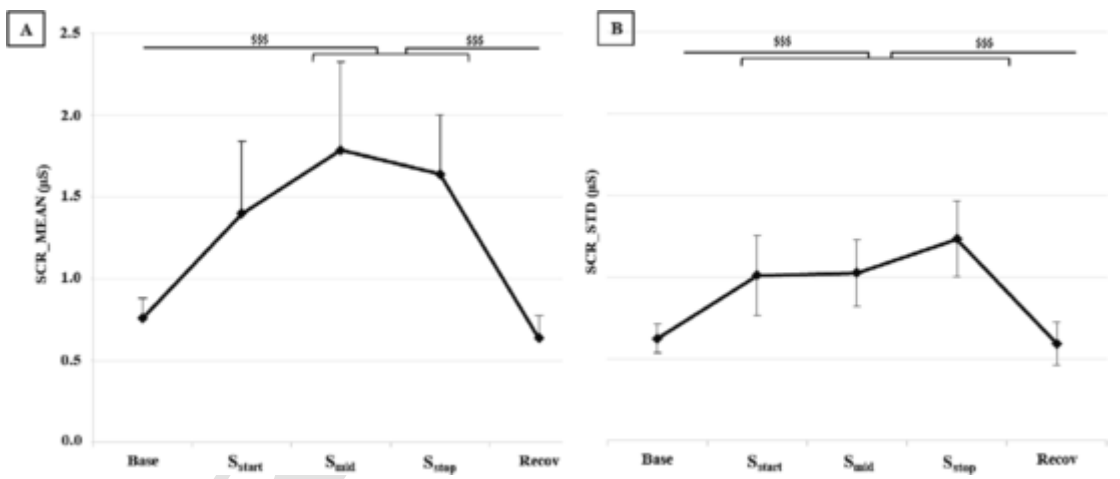

Fig. 11. (A) 'SCR_mean' and (B) 'SCR_std' values observed for each test period (Base, S_{start}, S_{mid}, S_{stop} and Recov) regardless of path predictability (mean ± SEM; n = 23). Statistical differences between test periods are shown in black. $$$ significant difference ($p < 0.001$).

Table 4
Results of (A) Pearson correlations between maximum CSR and physiological measurements and (B) Stepwise regression of physiological measurements on maximum CSR (Criterion to enter = 0.2). (n = 23) * $p < 0.05$ (two-tailed).

A	HR_mean	HR_std	In_max	Out_max	SCR_mean	SCR_std
CSR_max	0.466*	0.294*	0.359*	0.442*	0.171	-0.081

B	*β*	*t*	*Std. Error*	*p*
HR_mean	0.454	3.762	0.012	0.001
HR_std	0.238	1.860	0.054	0.070
Out_max	0.299	2.331	0.045	0.025

and 'In_max' (greater than 0.2 for both). These results suggest that the changes observed in cardiac and respiratory measurements and car-sickness symptoms are linked. In order to confirm this hypothesis, a regression analysis was performed to determine which physiological changes could be used to estimate maximum CSR during S_{max}. 'HR_mean', 'HR_std', 'In_max', and 'Out_max' showed adequate predictive power for inclusion in the regression. It was found that increases in car-sickness symptoms can be estimated from changes in cardiac and breathing activities. Indeed, 'HR_mean', 'HR_std', and 'Out_max' explained 41.4 % (adjusted $R2 = 0.372$) of the variance in maximum CSR values, ($F(3,42) = 9.899$, $\sigma est = 0.898$, $p < 0.001$) (Table 3B).

4. Discussion

For the first time in real driving conditions, our results show that sickness-inducing stimuli such as increased lateral acceleration and vehicle path unpredictability induce (i) an increase in symptom severity and (ii) specific physiological changes reflecting the activation of the SNS. CSR results reveal that the greater the lateral acceleration and the less predictable the vehicle path, the stronger the symptoms. Moreover, an increase in several physiological parameters is observed simultaneously with the increase in CSR, with moderate positive correlations between CSR evolution and physiological changes. Furthermore, linear regression results suggest that these physiological parameters can be used to detect car sickness, thus demonstrating a link between car sickness symptoms and physiological changes.

4.1. Triggers of car sickness

While the impact of acceleration in the vertical and longitudinal axes has been thoroughly documented, few studies have investigated the lateral axis. Yet lateral acceleration has been identified as the most nauseating in cars (Cheung & Nakashima, 2006; Diels, 2014; Smyth et al., 2021). Indeed, our finding that the higher the level of lateral acceleration, the stronger the car sickness symptoms extends those of previous work (Turner, 1999; Feng, 2017; Irmak, 2021), this time in the lateral axis and in real driving conditions. During the slalom period, participants exhibited a greater distribution of high CSR in High conditions than in Low conditions (RH: +75 % vs RL and UH: +39 % vs UL). In addition, participants recorded higher maximum CSR and reached this maximum earlier in High conditions (both Regular and Unpredictable) than in Low conditions. These results are consistent with previous findings on longitudinal acceleration. By increasing acceleration level in a dynamic simulator, Irmak et al. (2022) showed that maximum ratings not only increased but also were reached earlier, since their dropout rates increased. Regarding CSR dynamics, a significant increase was observed with time from S_{mid} onwards, reaching a maximum at 'S_{stop}'. Furthermore, the symptoms that developed during the slalom period, although attenuated, persisted into the recovery period ($CSR \neq 0$). These results extend results of previous papers showing that car sickness severity increases throughout testing (Kuiper et al., 2018; Irmak, 2021; Henry et al., 2022) and that symptoms can persist from minutes to hours after stimulation (Kim et al., 2005; Golding, 2006; Diels & Bos, 2016). However, we showed more specifically that high acceleration levels lead to a sharper increase in symptom severity, which remains higher during the post-stimulation recovery period. Our results demonstrate that there is a strong relationship between levels of lateral acceleration in cars and increased car sickness (timing and severity).

Determining what kind of lateral movements to avoid in future autonomous vehicles means exploring their separate impacts and parameters (acceleration, direction, frequency etc.). Our study employed the frequency known to induce maximum nausea in cars (Wada et al., 2012; Wada & Yoshida, 2016; Henry et al., 2022) regardless of acceleration level. Here, we show that increasing the level of acceleration in cars with sinusoidal lateral movements at this 0.2 Hz frequency leads to more severe symptoms. This extends results obtained with the Mc Cauley (1974) model applied to sinusoidal vertical movements (O'Hanlon & McCauley, 1974; Bos & Bles, 1998). At 0.2 Hz, Bos and Bles (1998) obtained more than 80 % MSI at 5 m/s², as opposed to around 60 % at 2 m/s². Our similar observations appear to suggest that acceleration level has a similar impact in the three axes (lateral, longitudinal, and vertical) at 0.2 Hz. Likely, the otolith tilt/translation ambiguity (Wood, 2002; Clément, 2011) induced at this 0.2 Hz frequency is amplified by the increase in acceleration level, whatever the direction of application. The vestibular system is known to be particularly sensitive to changes in velocity, i.e., accelerations (Mayne, 1974; Reason and Brand, 1975; Kuiper, Bos, Schmidt, et al., 2020b). When the acceleration level increases, the vestibular system thus becomes highly engaged and may be largely responsible for the worsening of the sensory conflict causing car sickness.

Our study also investigated, for the first time in real driving conditions, the impact of car path unpredictability on symptom severity. Interestingly, our results show that inability to predict vehicle path also exacerbates symptoms. Unpredictable conditions had a CSR distribution with more high scores than Regular conditions. More precisely, high scores appeared more frequently in UH conditions than in RH conditions at almost the same levels of acceleration (≈5m.s2). In addition, maximum CSR were greater in Unpredictable than in Regular at low acceleration levels. Furthermore, CSR were higher in 'S_{mid}' and 'S_{stop}' for UL conditions than for RL conditions and higher in 'S_{mid}' for UH conditions than for RH. Thus, inability to predict vehicle trajectories induced a gradual increase in symptom severity during the stimulation period. These results from real car lateral accelerations are in line with those obtained in the laboratory along the longitudinal axis using repeated fore-aft motion on a sled (Kuiper, Bos, Schmidt, et al., 2020b). Movements in response to events unpredictable either in timing or direction caused more severe motion sickness symptoms than when the same events occurred in a predictable way. In contrast, other studies on movement predictability have focused on the effectiveness of countermeasures allowing participants to anticipate future movements based on auditory (Kuiper, Bos, Diels, et al., 2020a; Maculewicz et al., 2021), visual (Hendricks & Tumpey, 1990) or multimodal cues (Sweeney & Bartell, 2017). Overall, they report less severe motion sickness symptoms when participants are able to anticipate future movements with help. However, these studies manipulated the par-

ticipants' ability to anticipate events, whereas our study manipulated the events themselves so as to make them unpredictable for the participants.

Nevertheless, both mechanisms depend on the updating of internal models according to the theory of sensory mismatch (Bos & Bles, 2002; Bos et al., 2008, 2010; Dennison et al., 2016). This theoretical framework explains why drivers do not experience motion sickness, whereas passengers do (Bos et al., 2008). Drivers can predict vehicle path (acceleration, speed, direction), which allows them to update their internal models and predict self-motion using efference copies (Reason and Brand, 1975; Bles et al., 1998; Bos & Bles, 1998; Bos et al., 2008). Typically, when the forward internal model is correctly tuned, the expected movements coincide with the perceived movements. Passengers however, in the absence of external help (anticipatory cues), are unable to predict upcoming movements. In addition, when passengers expect regular movements and the driver performs unpredictable movements, the mismatch between expected and real movements is amplified, and the internal model cannot be properly tuned. This may explain why our study found that participants became sicker in unpredictable conditions, consistent with the idea that a major cause of motion sickness is a mismatch between perceived and expected motion (Reason and Brand, 1975; Bles et al., 1998; Kuiper, Bos, Schmidt, et al., 2020b).

4.2. Physiological measures

As previously mentioned, the literature on physiological measurements and motion sickness indicates that (i) there is as yet no consensus on an objective indicator of motion sickness, (ii) despite the number of studies, there is no consensus on the directions (decrease/increase) of the physiological changes themselves, and (iii) so far, most studies have been conducted in laboratory conditions (rotating optokinetic drum, VR, Static driving simulator, etc.). Therefore, the third objective of this study was to investigate the relationship between car sickness and physiological responses in real driving conditions. We first analyzed the dynamics of physiological parameters retained over the several test phases to compare their evolution with CSR dynamics. Overall, the physiological parameters uniformly showed an significant evolution during the slalom period, whereas responses during the recovery period were not homogeneous.

'HR_mean' and 'HR_std' reflect modulations of cardiac activity and its variability during the test (Shaffer & Ginsberg, 2017; Meteier et al., 2021). 'HR_mean' showed a significant increase during the slalom period in all conditions and a return to baseline level only in Low and Regular conditions during the recovery period. This suggests that the most sickness-inducing conditions had the most persistent effects on cardiac activity. 'HR_std' showed an increase in High conditions during the slalom period, with a subsequent return to baseline level, indicating that changes were only induced by high levels of acceleration and did not persist over time. These increases could be interpreted as only due to the vehicle's movements and not to the evolution of the sickness. However, cardiac activity was elevated during the full slalom period, simultaneously with increased car sickness; for the most sickness-inducing stimuli, this persisted in the recovery period. Type of stimulation therefore has an impact on 'HR_mean' that may persist once the movements stop, indicating that the changes are not solely caused by the agitation experienced. Indeed, we observed a significant correlation between 'HR_mean', 'HR_std' values and the most severe car sickness (CSR_max): increases in car sickness severity were accompanied by increased cardiac activity. Our findings confirm the hypothesis of a relationship between car sickness and cardiac changes (Keshavarz et al., 2022), although findings in the literature remain inconsistent. This discrepancy is mainly due to the kind of stimuli employed, and/or the methodology used for measuring and analyzing cardiac activity. Several studies on cardiac parameters used laboratory setups, with inconclusive results (increase, decrease, no change) (Hu et al., 1991; Cheung, 2004; Kim et al., 2005; Dahlman et al., 2009; Koohestani et al., 2019). Only one study measured physiological variables in cars, reporting a slight increase in heart rate with car movements (Irmak, 2021). Yet the stimuli used were similar to those in our study, with a lateral acceleration of almost 4 m/s^2 (i.e., between our low and high conditions), and a condition with no view of the outside environment was used (i.e., highly sickness-inducing). Comparing our results with the literature reveals that the direction and magnitude of cardiac changes likely depends on the experimental environment and especially on the nature of the stimulus itself (frequency, acceleration, speed, direction).

Regarding RSP parameters, we analyzed maximum inspiration ('In_max') and expiration ('Out_max') values, reflecting respiratory volume. Although these features are not well documented in the literature, they proved relevant in our study. As with cardiac parameters, an increase in both was observed during the slalom period for all conditions. 'In_max' values revealed a gradual and strong increase until 'S_{stop}' in High conditions only, while 'Out_max' values exhibited the same pattern in RH conditions only. In the same vein, during the recovery period, respiratory measurements remained high only in High conditions for 'In_max' and in RH conditions for 'Out_max'. This provides evidence that higher lateral acceleration levels induce greater and more persistent changes in breathing volume. The positive correlation observed between our breathing parameters and the most severe car sickness (CSR_max) confirms this observation. This relationship is also supported by studies demonstrating that controlled breathing can reduce the level of motion sickness (Yen Pik Sang et al., 2003; Denise et al., 2009; Chin-Teng Lin et al., 2011). Lin et al., (2011) showed that people affected by motion sickness make breathing adjustments (deep breathing) to relieve their discomfort. However, in our study, while some increase in breathing volume was observed, these adjustments remained limited, mainly due to the car movements. In fact, we found that the frequency of car movements at 0.2 Hz imposed a specific respiration rate, which could partly explain why symptoms remained so severe: participants were not in full control of their breathing. Furthermore, in the regular conditions, participants could take advantage of periods with less stimulation (between turns) to adapt their breathing through greater inspiration and expiration. In contrast, our results tend to indicate that there were even fewer adjustments under unpredictable car movements, especially with high acceleration levels. All these observations argue for the hypothesis that physiological changes under sickness-inducing conditions depend on the nature of the stimulus.

Finally, we analyzed the EDA parameters 'SCR_mean' and 'SCR_std', the mean and variability of phasic skin conductance responses. This electrodermal conductance is used to measure sweating, a major motion sickness symptom (Kennedy et al., 2010; Lackner, 2014). Our SCR values increased during the slalom period and returned to baseline level during the recovery period. Under stimulation, 'SCR_mean' showed an increase from 'S_{mid}' to 'S_{stop}' and 'SCR_std' showed an increase from 'S_{start}' to S_{stop}'. These results are in agreement with those of Irmak et al. (2021), also obtained in a real car: sickness-inducing movements increased electrodermal conductance in palmar sites over time. The literature generally reports the same observation with increased severity of motion sickness (Hu et al., 1991; Harm, 2002; Kim et al., 2005). While it has been shown that forehead measurements gave highly sensitive measurements (Golding,1992; Wan & Hu, 2003), our results confirmed that measurements on palmar fingers also led to high satisfying sensibility. However, explanations for the underlying mechanisms remain unclear and inconsistent, possibly due to the varying measurement sites (forehead, finger, back of hand) and features used.

We observed several physiological changes when participants were affected by car sickness. There is a consensus among certain studies that all kinds of motion sickness can be considered as a stress response to a stressful stimulus (sickness-inducing movements) inducing particular physiological changes (Harm, 2002; Napoletano & Rossi, 2018). An increase in cardiovascular, respiratory, and/or electrodermal activities, as in our study, has previously been shown to reflect physiological stress (Cacioppo et al., 2007). It is known that depending on the stress or agitation level of the person, the homeostasis of the body is modulated, causing an alternation between the activation of the sympathetic and parasympathetic systems (Shaffer & Ginsberg, 2017). However, under severe stimulus, the sympathetic nervous system (SNS) dictates appropriate mechanisms and physiological responses to enhance the body's ability to deal with a threat (known as the "fight or flight response") (Harm, 2002; Irmak, 2021). Notably, this is achieved through increased arousal, which modifies electrodermal conductance (EDA), strongly correlated with the activity of the sweat glands (sweating) (Boucsein et al., 2012). It also increases the heart and respiratory rate, which amplifies the blood flow and enhances the transport and supply of oxygen in the body (Cacioppo et al., 2007; Chan et al., 2022). Therefore, our results seem to highlight a specific/dominant activation of the sympathetic system during the progression of car sickness symptoms. Nevertheless, motion sickness is more complex than a simple stress and/or agitation episode, which is why other studies contest the ability of physiological measurements alone to indicate motion sickness levels (Keshavarz et al., 2022; Smyth et al., 2021). Actually, the literature has illustrated the difficulty and unreliability of relating physiological measurements to motion sickness, depending on the environment and stimuli used (Dennison et al., 2016; Koohestani et al., 2019; Keshavarz et al., 2022). In our study, although the magnitude of our cardiac and respiratory changes depended on the stimuli used (4 conditions), all parameters evolved in the same direction and correlatively with car sickness severity. Moreover, the linear regression showed that our measures (cardiac and respiratory) could explain 41 % of the variance in maximum CSR values, demonstrating the link between the physiological state involved in car sickness and its symptoms.

4.3. Limitations of the study

Our results should be interpreted with caution in view of certain limitations. One major limitation of the study is sample size. Although the participants were selected for their high susceptibility to motion sickness, our results showed inter-individual variability which limited our data analyses (e.g., precise data temporal evolution, modeling, analysis per individual, etc.). More data from a heterogeneous and larger population are needed before these findings can be generalized. Second, this study is one of the first to measure physiological parameters in real driving conditions, which is both a limitation and a challenge. In our environment, where noise could impact the recorded data, the method of pre-processing and physiological feature extraction had to be adapted in order to obtain clean and useful signals. In addition, new physiological features not greatly affected by vehicle dynamics (respiration rate) were explored, reducing the scope for comparison with previous laboratory studies. However, our findings point to the value of common physiological measures, such as heart rate, already used in other motion sickness studies (Kim et al., 2005; Dahlman et al., 2009; Dennison et al., 2016; Koohestani et al., 2019; Irmak, 2021), as well as respiratory amplitude ('In_max' and 'Out_max'), as possible indicators of car sickness occurrence. These encouraging results deserve to be further explored. Third, it should be noted that when we manipulated vehicle path unpredictability, the acceleration level was also being manipulated. Under high acceleration levels, almost all participants rapidly reached their maximum symptoms (ratings of 4 = end of test). This saturation prematurely stopped the runs, resulting both in a rating plateau (a floor effect (Levine et al., 2014; Irmak, 2021)) and in reduced exposure time (≈10 min). Thus, had a higher symptom threshold than 'mild to moderate nausea' been applied, thereby lengthening exposure time, we might have observed a greater difference between the regular and unpredictable conditions even at high acceleration levels. Finally, only two lateral acceleration levels (2 m.s2 and 5 m.s2) and one frequency level (0.2 Hz) were analyzed in this study. Although this frequency is recognized in the literature as the most nauseating (Bos & Bles, 1998), and the lateral acceleration levels assessed here induced symptoms, this was not sufficient to allow proper analysis of the impact of vehicle dynamics in the different axes (lateral, longitudinal and vertical). Adapting the model proposed by Bos and Bles (1998) for vertical stimulations to car movements and determining the specific characteristics of movement causing car sickness will require testing a larger range of accelerations (0 to 6 m/s2) and frequencies (0 to 0.7 Hz). Once the impact of car movements is known, more realistic studies on the road should be considered.

5. Conclusion

For the first time in real driving conditions, our results show that the stronger the lateral acceleration (2 vs 5 m.s2), the more severe the symptoms of car sickness, and that inability to predict the vehicle's path exacerbates symptoms. In future autonomous vehicles, the vehicle dynamics will need to be designed, as far as possible, to limit nauseating movements such as high lateral acceleration and/or low frequency movements. In addition, countermeasure solutions should be considered to allow vehicle occupants to antici-

pate the vehicle's path in real time so as to update their internal model. Furthermore, these particular factors, which are highly prevalent during car travel, induce specific physiological changes reflecting SNS activation. It seems that the more impactful the stimulus is considered by participants (high CSR), the more their SNS is activated to allow the body to respond. Our work thus provides evidence that (i) physiological changes related to motion sickness can be recorded in the car with laboratory devices, (ii) processing stages need to be adapted according to these environmental constraints, (iii) some features explored in the laboratory can also be used in a real car, but (iv) new features (In_max and Out_max) also deserve to be explored and could reveal SNS activation. Indeed, the linear regression applied to our data suggests that these physiological parameters can be used to confirm the CSR level indicated by the participants. While the results of this study are encouraging, however, using physiological measures alone to indicate car sickness symptoms does not currently appear sufficient. Subjective measures such as ratings (CSR) still need to be used to evaluate car sickness severity and to identify the physiological changes associated with it. Automating the detection of car sickness from objective data only will require a predictive model taking into account the individuals' parameters as well as the nature of the stimuli. For this purpose, further research should be conducted to assess (i) the influence of other car-sickness-inducing factors (different vehicle dynamics, levels of control and predictability, passenger positioning, etc.) and (ii) the changes in individual parameters that these factors induce.

Uncited reference

Declaration of Competing Interest

The authors declare that they have no known competing financial interests or personal relationships that could have appeared to influence the work reported in this paper.

Data availability

The data that has been used is confidential.

Acknowledgments

We thank Julien Bonnet (Stellantis) and Aurore Bourrelly for their help in the preparation of this experiment. We are grateful to Telecom Paris Tech team as well as Rafik Belkacem and Nadjet Hosni for their technical assistance with data analysis. Finally, we thank Marjorie Sweetko for English language editing of the manuscript.

Funding

This study was conducted under a CIFRE thesis (N° 2018/1450 doctoral grant from National Association for Research and Technology (ANRT)) and the OpenLab agreement "Automotive Motion Lab" between Stellantis and Aix-Marseille University and CNRS.

Ethics Statement

This study was reviewed and approved by the Local Ethics Committee of Aix-Marseille University in accordance with the ethical standards laid down in the 1964 Declaration of Helsinki. The participants provided their written informed consent to participation in this study.

Author Contributions

All authors: Conceptualization, Methodology, Writing- Reviewing and Editing. Eléonore Henry and Clément Bougard: Investigation, Formal analysis and Visualization. Eléonore Henry : Data Curation, Writing- Original draft preparation. Clément Bougard, Christophe Bourdin and Lionel Bringoux Supervision.

Appendix A. Supplementary material

Supplementary data to this article can be found online at https://doi.org/10.1016/j.trf.2023.06.018.

References

Aykent, B., Merienne, F., Guillet, C., Paillot, D., & Kemeny, A. (2014). *Motion sickness evaluation and comparison for a static driving simulator and a dynamic driving simulator. Proceedings of the Institution of Mechanical Engineers, Part D: Journal of Automobile Engineering, 228*(7), 818–829. https://doi.org/10.1177/0954407013516101.

Benedek, M., & Kaernbach, C. (2010). *Decomposition of skin conductance data by means of nonnegative deconvolution. Psychophysiology, 47*(4), 647–658. https://doi.org/10.1111/j.1469-8986.2009.00972.x.

Bles, W., Bos, J.E., de Graaf, B., Groen, E., & Wertheim, A.H. (1998). *Motion sickness : Only one provocative conflict? Brain Research Bulletin, 47*(5), 481–487. https://doi.org/10.1016/S0361-9230(98)00115-4.

Bos, J.E., & Bles, W. (1998). *Modelling motion sickness and subjective vertical mismatch detailed for vertical motions. Brain Research Bulletin, 47*(5), 537–542. https://

doi.org/10.1016/S0361-9230(98)00088-4.
Bos, J.E., & Bles, W. (2002). *Theoretical considerations on canal–otolith interaction and an observer model. Biological Cybernetics*, *86*(3), 191–207. https://doi.org/10.1007/s00422-001-0289-7.
Bos, J. E., Bles, W., & Groen, E. L. (2008). *A theory on visually induced motion sickness*. 11.
Bos, J.E., de Vries, S.C., van Emmerik, M.L., & Groen, E.L. (2010). *The effect of internal and external fields of view on visually induced motion sickness*. *Applied Ergonomics*, *41*(4), 516–521. https://doi.org/10.1016/j.apergo.2009.11.007.
Bos, J., Mackinnon, S., & Patterson, A. (2006). *Motion Sickness Symptoms in a Ship Motion Simulator : Effects of Inside, Outside and No View*. *Aviation, space, and environmental medicine*, *76*, 1111–1118.
Bos, J.E., Van Leeuwen, R.B., & Bruintjes, T.D. (2018). *Motion sickness in motion: From carsickness to cybersickness*. *Nederlands tijdschrift voor geneeskunde*, *162*, D1760–D.
Boucsein, W. (2012). Principles of Electrodermal Phenomena. In W. Boucsein (Éd.), *Electrodermal Activity* (p. 1-86). Springer US. Doi: 10.1007/978-1-4614-1126-0_1.
Cacioppo, J., Tassinary, L., & Berntson, G. (2007). *Handbook of psychophysiology*. https://doi.org/10.13140/2.1.2871.1369.
Carreiras, C., Alves, A.P., Lourenço, A., Canento, F., Silva, H., & Fred, A. (2015). *Biosppy : Biosignal processing in python*. *Accessed on*, *3*(28), 2018.
Chan, P.Y., Ryan, N.P., Chen, D., McNeil, J., & Hopper, I. (2022). *Novel wearable and contactless heart rate, respiratory rate, and oxygen saturation monitoring devices : A systematic review and meta-analysis*. *Anaesthesia*, *77*(11), 1268–1280. https://doi.org/10.1111/anae.15834.
Chen, Y.-C., Duann, J.-R., Chuang, S.-W., Lin, C.-L., Ko, L.-W., Jung, T.-P., & Lin, C.-T. (2010). *Spatial and temporal EEG dynamics of motion sickness*. *NeuroImage*, *49*(3), 2862–2870. https://doi.org/10.1016/j.neuroimage.2009.10.005.
Cheung, B. (2004). Physiological and behavioral responses to an exposure of pitch illusion in the simulator. Aviation, space, and environmental medicine. (75)8. P.657. https://sh2hh6qx2e.search.serialssolutions.com/?sid=google&auinit=B&aulast=Cheung&atitle=Physiological+and+behavioral+responses+to+an+exposure+of+pitch+illusion+in+the+simulator&title=Aviation,+space,+and+environmental+medicine&volume=75&issue=8&date=2004&spage=657&issn=0095-6562.
Cheung, B., & Nakashima, A. (2006). *A Review on the Effects of Frequency of Oscillation on Motion Sickness*. 29.
Lin, C.-T., Lin, C.-L., Chiu, T.-W., Duann, J.-R., & Jung, T.-P. (2011). *Effect of respiratory modulation on relationship between heart rate variability and motion sickness*. *Annual International Conference of the IEEE Engineering in Medicine and Biology Society*, *2011*, 1921–1924. https://doi.org/10.1109/IEMBS.2011.6090543.
Clément, G. (2011). *Fundamentals of Space Medicine*. *Springer, New York*. https://doi.org/10.1007/978-1-4419-9905-4.
Dahlman, J., Sjörs, A., Lindström, J., Ledin, T., & Falkmer, T. (2009). *Performance and Autonomic Responses During Motion Sickness*. *Human Factors: The Journal of the Human Factors and Ergonomics Society*, *51*(1), 56–66. https://doi.org/10.1177/0018720809332848.
Denise, P., Vouriot, A., Normand, H., Golding, J.F., & Gresty, M.A. (2009). *Effect of temporal relationship between respiration and body motion on motion sickness*. *Autonomic Neuroscience*, *151*(2), 142–146. https://doi.org/10.1016/j.autneu.2009.06.007.
Dennison, M.S., Wisti, A.Z., & D'Zmura, M. (2016). *Use of physiological signals to predict cybersickness*. *Displays*, *44*, 42–52. https://doi.org/10.1016/j.displa.2016.07.002.
Diels, C. (2014). Will autonomous vehicles make us sick? In S. Sharples & S. Shorrock (Éds.), *Contemporary Ergonomics and Human Factors 2014* (p. 301-307). Taylor & Francis. Doi: 10.1201/b16742-56.
Diels, C., & Bos, J.E. (2016). *Self-driving carsickness*. *Applied Ergonomics*, *53*, 374–382. https://doi.org/10.1016/j.apergo.2015.09.009.
Donohew, B.E., & Griffin, M.J. (2004). *Motion Sickness : Effect of the Frequency of Lateral Oscillation.*, *75*(8), 8.
Feenstra, P.J., Bos, J.E., & van Gent, R.N.H.W. (2011). *A visual display enhancing comfort by counteracting airsickness*. *Displays*, *32*(4), 194–200. https://doi.org/10.1016/j.displa.2010.11.002.
Feng, F. (2017). *Can vehicle longitudinal jerk be used to identify aggressive drivers ? An examination using naturalistic driving data. Accident Analysis and Prevention*, *12*.
Gavgani, A.M., Nesbitt, K.V., Blackmore, K.L., & Nalivaiko, E. (2017). *Profiling subjective symptoms and autonomic changes associated with cybersickness*. *Autonomic Neuroscience*, *203*, 41–50. https://doi.org/10.1016/j.autneu.2016.12.004.
Gianaros, P.J., Quigley, K.S., Muth, E.R., Levine, M.E., Vasko, R.C., Jr., & Stern, R.M. (2003). *Relationship between temporal changes in cardiac parasympathetic activity and motion sickness severity*. *Psychophysiology*, *40*(1), 39–44. https://doi.org/10.1111/1469-8986.00005.
Golding, J.F. (2006). *Motion sickness susceptibility*. *Autonomic Neuroscience*, *129*(1–2), 67–76. https://doi.org/10.1016/j.autneu.2006.07.019.
Golding, J.F., Mueller, A.G., & Gresty, M.A. (2001). *A motion sickness maximum around the 0.2 Hz frequency range of horizontal translational oscillation. Aviation, Space, and Environmental Medicine*, *72*(3), Article 3.
Green, P. (2016). *Motion Sickness and Concerns for Self-Driving Vehicles : A Literature. Review.*, *83*.
Griffin, M.J., & Newman, M.M. (2004). *An experimental study of low-frequency motion in cars*. *Proceedings of the Institution of Mechanical Engineers, Part D: Journal of Automobile Engineering*, *218*(11), 1231–1238. https://doi.org/10.1243/0954407042580093.
Harm, D.L. (2002). *Motion Sickness Neurophysiology*. *Physiological Correlates, and Treatment.*, *29*.
Hendricks, R., & Tumpey, T. (1990). *Contribution of virus and immune factors to herpes simplex virus type I-induced corneal pathology. Investigative ophthalmology & visual science*, *31*, 1929–1939.
Henry, E.H., Bougard, C., Bourdin, C., & Bringoux, L. (2022). *Changes in Electroencephalography Activity of Sensory Areas Linked to Car Sickness in Real Driving Conditions*. *Frontiers in Human Neuroscience*, *15*. https://www.frontiersin.org/articles/10.3389/fnhum.2021.809714.
Himi, N., Koga, T., Nakamura, E., Kobashi, M., Yamane, M., & Tsujioka, K. (2004). *Differences in autonomic responses between subjects with and without nausea while watching an irregularly oscillating video*. *Autonomic Neuroscience*, *116*(1–2), 46–53. https://doi.org/10.1016/j.autneu.2004.08.008.
Hu, S., Grant, W.F., Stern, R.M., & Koch, K.L. (1991). *Motion sickness severity and physiological correlates during repeated exposures to a rotating optokinetic drum. Aviation, Space, and Environmental Medicine*, *62*, 308–314.
Irmak, T. (2021). *Objective and subjective responses to motion sickness : The group and the individual. Experimental Brain Research*, *17*.
Islam, R., Lee, Y., Jaloli, M., Muhammad, I., Zhu, D., & Quarles, J. (2020). *Automatic Detection of Cybersickness from Physiological Signal in a Virtual Roller Coaster Simulation.* https://doi.org/10.1109/VRW50115.2020.00175.
Kennedy. (1993). *Kennedy et al, 1993 Simulator sickness questionnaire : An enhanced method for quantifying simulator sickness*.
Kennedy, R.S., Drexler, J., & Kennedy, R.C. (2010). *Research in visually induced motion sickness*. *Applied Ergonomics*, *41*(4), 494–503. https://doi.org/10.1016/j.apergo.2009.11.006.
Keshavarz, B., Peck, K., Rezaei, S., & Taati, B. (2022). *Detecting and predicting visually induced motion sickness with physiological measures in combination with machine learning techniques*. *International Journal of Psychophysiology*, *176*, 14–26. https://doi.org/10.1016/j.ijpsycho.2022.03.006.
Kim, J., & Park, T. (2020). *The Onset Threshold of Cybersickness in Constant and Accelerating Optical Flow*. *Applied Sciences*, *10*(21), 7808. https://doi.org/10.3390/app10217808.
Kim, Y. Y., Kim, H. J., Kim, E. N., Ko, H. D., & Kim, H. T. (2005). Characteristic changes in the physiological components of cybersickness. *Psychophysiology*, *0*(0), 050826083901001-??? Doi: 10.1111/j.1469-8986.2005.00349.x.
Koohestani, A., Nahavandi, D., Asadi, H., Kebria, P.M., Khosravi, A., Alizadehsani, R., & Nahavandi, S. (2019). *A Knowledge Discovery in Motion Sickness : A Comprehensive Literature Review*. *IEEE Access*, *7*, 85755–85770. https://doi.org/10.1109/ACCESS.2019.2922993.
Kuiper, O.X., Bos, J.E., & Diels, C. (2018). *Looking forward : In-vehicle auxiliary display positioning affects carsickness*. *Applied Ergonomics*, *68*, 169–175. https://doi.org/10.1016/j.apergo.2017.11.002.
Kuiper, O.X., Bos, J.E., Diels, C., & Schmidt, E.A. (2020). *Knowing what's coming : Anticipatory audio cues can mitigate motion sickness*. *Applied ergonomics*, *85*, 103068.
Kuiper, O.X., Bos, J.E., Schmidt, E.A., Diels, C., & Wolter, S. (2020). *Knowing What's Coming : Unpredictable Motion Causes More Motion Sickness*. *Human Factors: The Journal of the Human Factors and Ergonomics Society*, *62*(8), 1339–1348. https://doi.org/10.1177/0018720819876139.
Lackner, J.R. (2014). *Motion sickness : More than nausea and vomiting. Experimental Brain Research*, *232*(8), 2493–2510. https://doi.org/10.1007/s00221-014-4008-8.
LaCount, L., Napadow, V., Kuo, B., Park, K., Kim, J., Brown, E., & Barbieri, R. (2009). *Dynamic Cardiovagal Response to Motion Sickness : A Point-Process Heart Rate Variability Study*. 4.
LaCount, L.T., Barbieri, R., Park, K., Kim, J., Brown, E.N., Kuo, B., & Napadow, V. (2011). *Static and Dynamic Autonomic Response with Increasing Nausea Perception.*

Aviation, space, and environmental medicine, *82*(4), 424–433.
Lawther, A., & Griffin, M.J. (1987). *Prediction of the incidence of motion sickness from the magnitude, frequency, and duration of vertical oscillation. J. Acoust. Soc. Am.*, *82* (3), 10.
Levine, M.E., Stern, R.M., & Koch, K.L. (2014). *Enhanced perceptions of control and predictability reduce motion-induced nausea and gastric dysrhythmia. Experimental brain research*, *232*(8), 2675–2684.
Li, G., & Chung, W.-Y. (2013). *Detection of Driver Drowsiness Using Wavelet Analysis of Heart Rate Variability and a Support Vector Machine Classifier*. *Sensors*, *13*(12), Article 12. https://doi.org/10.3390/s131216494.
Lin, C.-T., Chuang, S.-W., Chen, Y.-C., Ko, L.-W., Liang, S.-F., & Jung, T.-P. (2007). EEG Effects of Motion Sickness Induced in a Dynamic Virtual Reality Environment. *2007 29th Annual International Conference of the IEEE Engineering in Medicine and Biology Society* (pp. 3872–3875). https://doi.org/10.1109/IEMBS.2007.4353178.
Maculewicz, J., Larsson, P., & Fagerlönn, J. (2021). *Intuitive and subtle motion-anticipatory auditory cues reduce motion sickness in self-driving cars.*, *23*.
Makowski, D. (2016). Neurokit : A python toolbox for statistics and neurophysiological signal processing (eeg, eda, ecg, emg...). *Memory and Cognition Lab'Day*, *1*.
Mayne. (1974). *A Systems Concept of the Vestibular Organs | SpringerLink*. https://link.springer.com/chapter/10.1007/978-3-642-65920-1_14.
Meteier, Q., Capallera, M., Ruffieux, S., Angelini, L., Abou Khaled, O., Mugellini, E., … Sonderegger, A. (2021). *Classification of Drivers' Workload Using Physiological Signals in Conditional Automation*. *Frontiers in Psychology*, *12*, 596038. https://doi.org/10.3389/fpsyg.2021.596038.
Money, K.E. (1970). *Motion sickness*. *Physiological Reviews*, *50*(1), 1–39. https://doi.org/10.1152/physrev.1970.50.1.1.
Mühlbacher, D., Tomzig, M., Reinmüller, K., & Rittger, L. (2020). *Methodological Considerations Concerning Motion Sickness Investigations during Automated Driving*. *Information*, *11*(5), 265. https://doi.org/10.3390/info11050265.
Muth, E.R. (2006). *Motion and space sickness : Intestinal and autonomic correlates*. *Autonomic Neuroscience*, *129*(1–2), 58–66. https://doi.org/10.1016/j.autneu.2006.07.020.
Nalivaiko, E., Davis, S.L., Blackmore, K.L., Vakulin, A., & Nesbitt, K.V. (2015). *Cybersickness provoked by head-mounted display affects cutaneous vascular tone, heart rate and reaction time*. *Physiology & Behavior*, *151*, 583–590. https://doi.org/10.1016/j.physbeh.2015.08.043.
Napoletano, P., & Rossi, S. (2018). Combining heart and breathing rate for car driver stress recognition. *2018 IEEE 8th International Conference on Consumer Electronics - Berlin (ICCE-Berlin)*, 1-5. Doi: 10.1109/ICCE-Berlin.2018.8576164.
Naqvi, S.A.A., Badruddin, N., Jatoi, M.A., Malik, A.S., Hazabbah, W., & Abdullah, B. (2015). *EEG based time and frequency dynamics analysis of visually induced motion sickness (VIMS)*. *Australasian Physical & Engineering Sciences in Medicine*, *38*(4), 721–729. https://doi.org/10.1007/s13246-015-0379-9.
Nunan, D., Sandercock, G. R. H., & Brodie, D. A. (2010). A Quantitative Systematic Review of Normal Values for Short-Term Heart Rate Variability in Healthy Adults : REVIEW OF SHORT-TERM HRV VALUES. *Pacing and Clinical Electrophysiology*, *33*(11), 1407-1417. Doi: 10.1111/j.1540-8159.2010.02841.x.
O'Hanlon, J. F., & McCauley, M. E. (1974). Motion sickness incidence as a function of the frequency and acceleration of vertical sinusoidal motion. *Aerospace Medicine*, *45*(4), 366-369.
Ohyama, S., Nishiike, S., Watanabe, H., Matsuoka, K., Akizuki, H., Takeda, N., & Harada, T. (2007). *Autonomic responses during motion sickness induced by virtual reality*. *Auris Nasus Larynx*, *34*(3), 303–306. https://doi.org/10.1016/j.anl.2007.01.002.
Perrin, P., Lion, A., Bosser, G., Gauchard, G., & Meistelman, C. (2013). *Motion Sickness in Rally Car Co-Drivers*. *Aviation, Space, and Environmental Medicine*, *84*(5), 473–477. https://doi.org/10.3357/ASEM.3523.2013.
Pukhova, V., Gorelova, E., Ferrini, G., & Burnasheva, S. (2017). *Time-frequency representation of signals by wavelet transform. IEEE Conference of Russian Young Researchers in Electrical and Electronic Engineering (EIConRus)*, *2017*, 715–718. https://doi.org/10.1109/EIConRus.2017.7910658.
Reason, J.T. (1978). *Motion Sickness Adaptation : A Neural Mismatch Model*. *Journal of the Royal Society of Medicine*, *71*(11), 819–829. https://doi.org/10.1177/014107687807101109.
Reason, J. T., & Brand, J. J. (1975). *Motion sickness* (p. vii, 310). Academic Press.
Rolnick, A., & Lubow, R.E. (1991). *Why is the driver rarely motion sick? The role of controllability in motion sickness*. *Ergonomics*, *34*(7), 867–879. https://doi.org/10.1080/00140139108964831.
Salahuddin, L., Cho, J., Jeong, M. G., & Kim, D. (2007, August). Ultra short term analysis of heart rate variability for monitoring mental stress in mobile settings. In 2007 29th annual international conference of the ieee engineering in medicine and biology society (pp. 4656-4659). IEEE. Doi: 10.1109/IEMBS.2007.4353378.
Salter, S., Diels, C., Herriotts, P., Kanarachos, S., & Thake, D. (2019). *Motion sickness in automated vehicles with forward and rearward facing seating orientations*. *Applied Ergonomics*, *78*, 54–61. https://doi.org/10.1016/j.apergo.2019.02.001.
Schmidt, E.A., Kuiper, O.X., Wolter, S., Diels, C., & Bos, J.E. (2020). *An international survey on the incidence and modulating factors of carsickness*. *Transportation Research Part F: Traffic Psychology and Behaviour*, *71*, 76–87. https://doi.org/10.1016/j.trf.2020.03.012.
Sclocco, R., Kim, J., Garcia, R.G., Sheehan, J.D., Beissner, F., Bianchi, A.M., … Napadow, V. (2016). *Brain Circuitry Supporting Multi-Organ Autonomic Outflow in Response to Nausea*. *Cerebral Cortex*, *26*(2), 485–497. https://doi.org/10.1093/cercor/bhu172.
Shaffer, F., & Ginsberg, J.P. (2017). *An Overview of Heart Rate Variability Metrics and Norms*. *Frontiers in Public Health*, *5*, 258. https://doi.org/10.3389/fpubh.2017.00258.
Shoeb, A., & Clifford, G. (2005). *Chapter 16—Wavelets; Multiscale Activity in Physiological Signals*. http://www.mit.edu/~gari/teaching/6.555/LECTURE_NOTES/wavelet_lecture_notes.pdf.
Sivak, M., & Schoettle, B. (2015). *MOTION SICKNESS IN SELF-DRIVING VEHICLES*. 15.
Smyth, J., Jennings, P., Bennett, P., & Birrell, S. (2021). *A novel method for reducing motion sickness susceptibility through training visuospatial ability – A two-part study*. *Applied Ergonomics*, *90*, 103264. https://doi.org/10.1016/j.apergo.2020.103264.
Sweeney, M. and Bartell, E. (2017). *Sensory Stimulation System for an Autonomous Vehicle, US20170313326, U.S. Patent and Trademark Office, Washington, DC.*
Taylor, S., Jaques, N., Chen, W., Fedor, S., Sano, A., & Picard, R. (2015). Automatic identification of artifacts in electrodermal activity data. *2015 37th Annual International Conference of the IEEE Engineering in Medicine and Biology Society (EMBC)*, 1934-1937. Doi: 10.1109/EMBC.2015.7318762.
Turner, M. (1999). Motion sickness in public road transport : Passenger behaviour and susceptibility. *Ergonomics*, *42*(3), 444-461. Doi: 10.1080/001401399185586.
Wada, T., Fujisawa, S., & Doi, S. (2018). *Analysis of driver's head tilt using a mathematical model of motion sickness*. *International Journal of Industrial Ergonomics*, *63*, 89–97. https://doi.org/10.1016/j.ergon.2016.11.003.
Wada, T., Konno, H., Fujisawa, S., & Doi, S. (2012). *Can Passengers' Active Head Tilt Decrease the Severity of Carsickness? : Effect of Head Tilt on Severity of Motion Sickness in a Lateral Acceleration Environment*. *Human Factors: The Journal of the Human Factors and Ergonomics Society*, *54*(2), 226–234. https://doi.org/10.1177/0018720812436584.
Wada, T., & Yoshida, K. (2016). *Effect of passengers' active head tilt and opening/closure of eyes on motion sickness in lateral acceleration environment of cars*. *Ergonomics*, *59* (8), 1050–1059. https://doi.org/10.1080/00140139.2015.1109713.
Wood, S.J. (2002). *Human otolith–ocular reflexes during off-vertical axis rotation : Effect of frequency on tilt–translation ambiguity and motion sickness*. *Neuroscience Letters*, *323*(1), 41–44. https://doi.org/10.1016/S0304-3940(02)00118-0.
Yen Pik Sang, F., Golding, J. F., & Gresty, M. A. (2003). Suppression of sickness by controlled breathing during mildly nauseogenic motion. *Aviation, Space, and Environmental Medicine*, *74*(9), Article 9.